

ANGULAR DISTRIBUTIONS AND ANISOTROPY OF THE FISSION FRAGMENTS FROM NEUTRON-INDUCED FISSION OF ^{233}U AND ^{209}Bi IN INTERMEDIATE ENERGY RANGE 1–200 MEV

A.S. Vorobyev¹, A.M. Gagarski¹, O.A. Shcherbakov¹, L.A. Vaishnene¹, A.L. Barabanov^{2,3}

¹*NRC “Kurchatov Institute”, B.P. Konstantinov Petersburg Nuclear Physics Institute, 188300, Gatchina, Leningrad district, Russia*

²*NRC “Kurchatov Institute”, 123182, Moscow, Russia*

³*Moscow Institute of Physics and Technology, 141700, Dolgoprudny, Moscow Region, Russia*

Abstract

New results of the neutron-induced fission experiments carried out at the neutron time-of-flight spectrometer GNEIS of the PNPI are given. Angular distributions of fission fragments from the neutron-induced fission of ^{233}U and ^{209}Bi nuclei have been measured in the energy range 1–200 MeV using position sensitive multiwire proportional counters as fission fragment detector. The data on anisotropy of fission fragments deduced from the measured angular distributions are presented in comparison with the experimental data of other authors.

1. Introduction

Angular distributions of fission fragments arise due to two factors. First, an ensemble of spins of fissioning nuclei is to be aligned and, second, distribution of transitional states over the K projection of nuclear spin on the fission axis should be nonuniform. The first factor is determined by the processes, which precede to fission, while the latter one is given by the mechanism of fission. At the energies much exceeding the fission barrier, the fission is preceded by the multi-step particle emission. A relative contribution of equilibrium and nonequilibrium processes into the dynamics of highly excited nuclei is not clear up to now. The angular distribution of fragments from neutron-induced fission at the energies up to 200 MeV may shed some light on these questions. Besides, the data on nuclear fission in this intermediate energy range are of prime importance for the advanced nuclear technologies such as Accelerator-Driven Systems (for nuclear power generation and nuclear transmutation).

We present here the results of measurements which continue the neutron-induced fission experiments at the neutron time-of-flight (TOF) spectrometer GNEIS [1] of the PNPI. In the previous paper [2] we have reported the data on angular anisotropy of fragments from neutron-induced fission of the target nuclei of ^{235}U , ^{238}U and ^{232}Th in the intermediate energy range 1–200 MeV. The data for ^{235}U nucleus are of special interest due to, first, a significance of ^{235}U as a fuel element and, second, the fact that similar measurements recently were made at n_TOF [3,4] and LANSCE [5] facilities.

The situation with the other important fuel element, ^{233}U , is quite different. Up to now there were no experimental data on the fragment's angular anisotropy for incident neutrons above 24 MeV (this is the upper limit of the rather old measurement of Simmons and Henkel [6]). In this paper the results of our study of the angular distribution of fragments from fission of ^{233}U nuclei by neutrons with the energies 1–200 MeV are presented.

Besides actinides, bismuth and lead are of interest due to their role in current and future nuclear power technologies. Lead-bismuth eutectic (alloy) is one of the primary coolant candidates for advanced nuclear reactors and Accelerator-Driven System. In addition to, this alloy is proposed as a target material for high power spallation neutron sources of new

generation. Bismuth is also considered as a possible candidate to be used as a secondary standard for the cross section of neutron-induced fission because it is a mono isotope with a fission threshold about 40 MeV. In this paper new experimental data on the angular anisotropy of fragments from fission of ^{209}Bi nuclei by neutrons up to 200 MeV are given.

During the last two decades, the neutron-induced fission cross section of ^{209}Bi nuclei has been measured few times at the intermediate energies up to 1 GeV using both “white” and quasi-monoenergetic neutron sources. The data on fission cross section obtained by different authors are in a satisfactory agreement with each other. However, only one measurement of fragment angular anisotropy has been performed with the use of quasi-monoenergetic neutrons of 75 MeV at The Svedberg Laboratory by Eismont et al. [7]. Thus our work is a first attempt to study the energy dependence of the fragment's angular anisotropy for ^{209}Bi .

2. General description of the experimental set-up

A schematic view of the experimental set-up is shown in Figs. 1, 2. Detailed description of the set-up and readout system created on the basis of waveform digitizers can be found in our previous publication [2].

The metal ^{209}Bi target $120 \times 120 \text{ mm}^2$ of size was made by vacuum deposition of ^{209}Bi on $2 \mu\text{m}$ Mylar foil. The ^{233}U target $50 \times 70 \text{ mm}^2$ of size was made by painting technique with U_3O_8 -deposit on $100 \mu\text{m}$ Al foil. The target thicknesses were about $1000 \mu\text{g}/\text{cm}^2$ and $150 \mu\text{g}/\text{cm}^2$, respectively. The fission fragment registration was performed by two coordinates sensitive multiwire proportional counters (MWPC) $140 \times 140 \text{ mm}^2$ of size [8]. The fragment counters were placed close to the target in the beam one after the other. The neutron beam axis came through the geometrical centers of the target and MWPC's electrodes being perpendicular to them. In order to have a possibility to take into account for the linear momentum contribution into the measured angular distribution the measurements with two set-up orientations relative to the beam direction (downstream and upstream) were performed.

A value of $\cos(\theta)$, where θ is an angle between neutron beam axis and fission fragment momentum, can be derived easily from the coordinates of the fission fragment measured by two counters. Time and pulse-height analysis of the signal waveforms allowed to derive the neutron energy and the fission fragment coordinates, and, hence, the angle information.

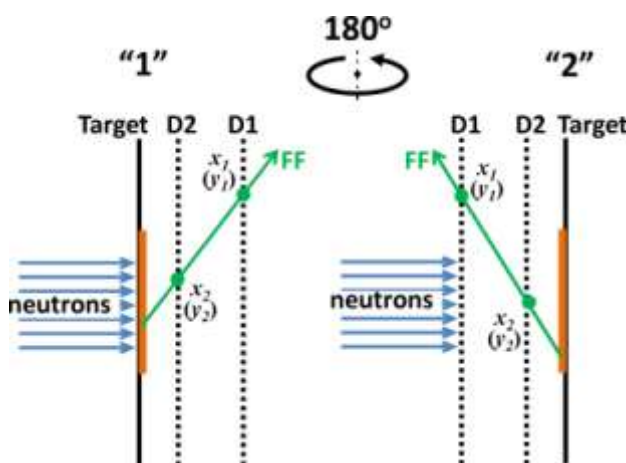


Fig. 1. Schematic view of the experimental set-up at two orientation relative to the neutron beam direction (downstream and upstream).

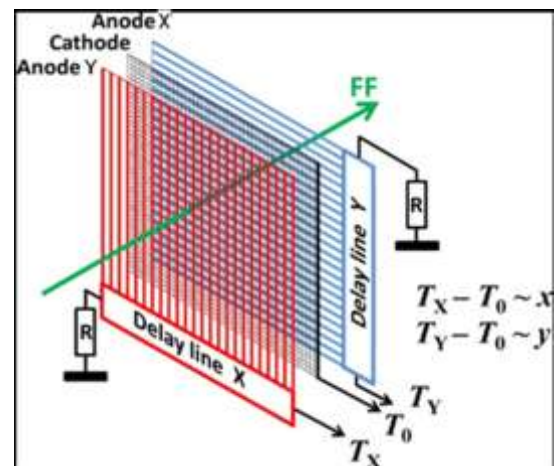


Fig. 2. Construction of the MWPC and principle of the coordinate determination.

3. Data processing

The main advantage of the present experimental set-up is that the efficiency of fission fragment registration is completely determined by the geometry of the MWPC. Indeed, the efficiency is limited only by the geometrical transparency of the wire electrodes of MWPC since the fragments pass throughout the MWPC without any significant energy loss in the target backing, the electrode planes or the working gas. To realize this advantage, one needs to separate “useful” fission events from “corrupted” events. The latter are caused by the fragments which do not reach the last wire electrode owing to absorption in the previous wire plane and by the non-fission reaction products. In the present measurements, we used in addition to our previous work [2] the selection criteria (or lines) in three two-dimensional correlation plots:

- a correlation between $\cos(\theta)$ and the amplitude of the Y-anode signal of the MWPC 2 (shown in Fig.1 as D2) is plotted in Fig. 3 together with the separation line (black curve), the events above this separation line are taken as fission events;
- a correlation between $\cos(\theta)$ and the amplitude of the X-anode signal of the MWPC 2, the selection criterion similar to that for Y-anode signal is used;
- a correlation between amplitudes of the X-anode signals from two MWPCs is presented in Fig. 4 together with the separation line (black straight line); the events to the left from this separation line should be attributed to the fission fragments which did not reach the last anode (X-anode of MWPC 1, shown in Fig. 1 as D1) because they hit the wires of the last cathode plane, such events were discarded.

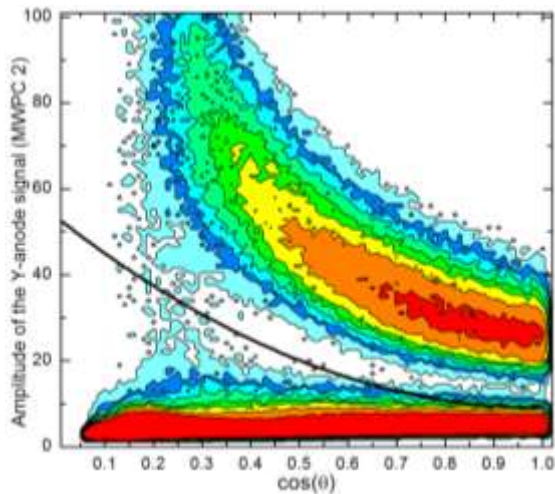


Fig. 3. Dependence of the amplitude of the Y-anode signal of MWPC 2 (D2) on the angle between fission fragment momentum and normal to the anode plane (^{233}U). The “useful” events are located above the separation line (black).

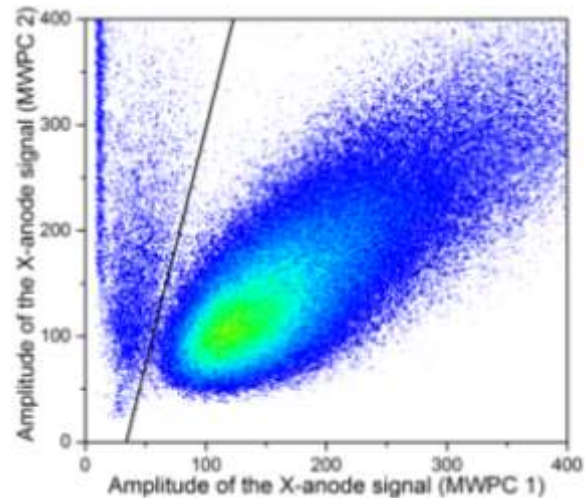


Fig. 4. Correlation between amplitudes of the X-anode signals of two MWPCs (^{233}U). The “useful” events are located to the right of the separation line.

To demonstrate the selectivity effectiveness of applied procedure, the two-dimensional plots of the amplitudes of correlated cathode signals from two MWPCs are shown in Figs. 5,6 (for ^{233}U and ^{209}Bi case, respectively) for all events and for “useful” events selected by means of the described procedure.

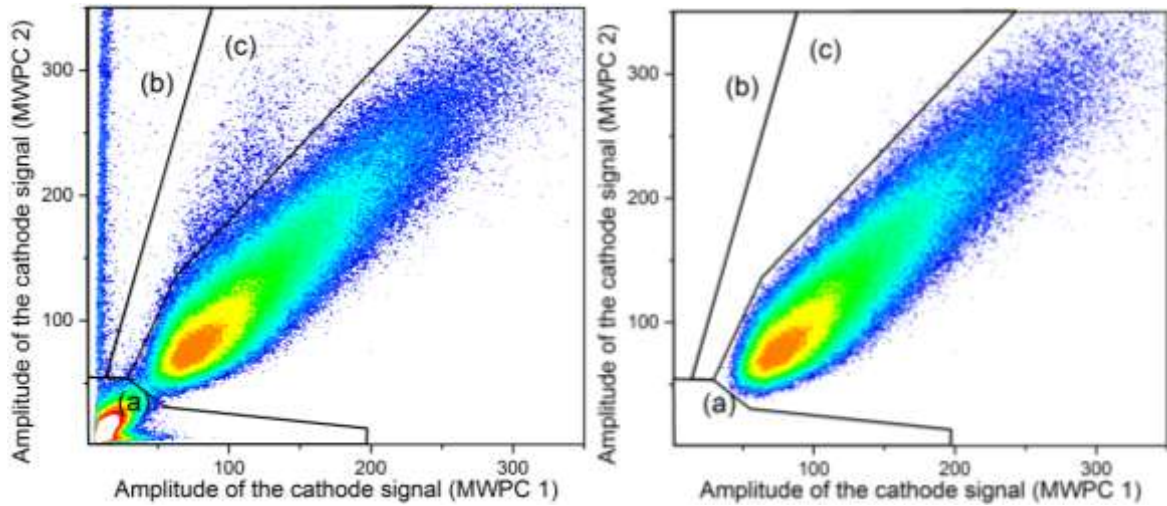


Fig. 5. A two-dimensional plot of the amplitudes of the cathode signals from two MWPCs in ^{233}U experiment. The area of non-fission reaction products is labeled as (a). The fission events produced in the target are labeled: (b) - if fission fragments do not reach MWPC 1 (D1) due to limited transparency of MWPC 2 (D2); (c) - if the fragments do not pass through the cathode of the MWPC 1 (D1). Right part of this figure shows only “useful” data (for explanation see the text).

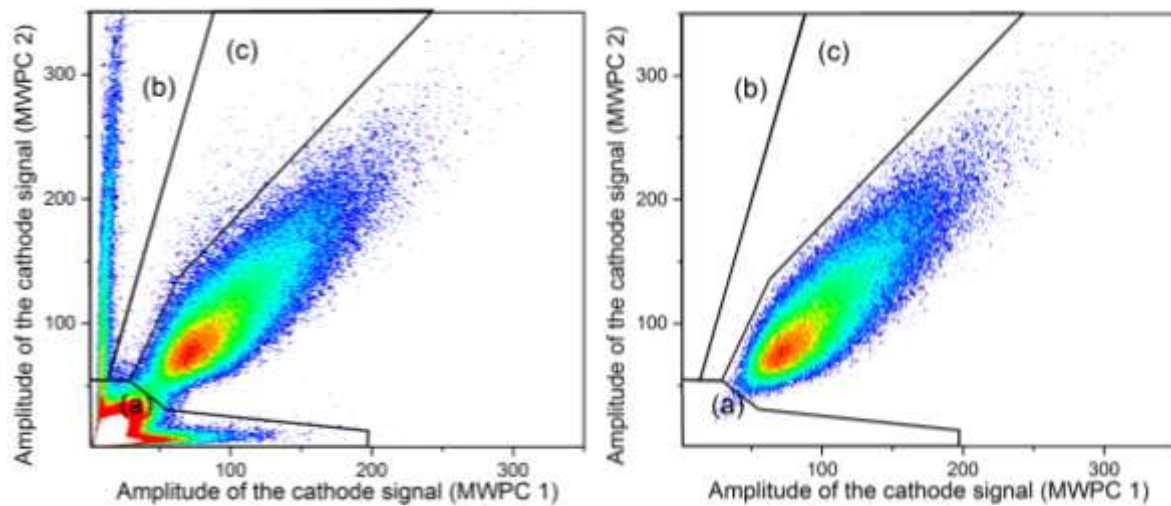


Fig. 6. A two-dimensional plot of the amplitudes of the cathode signals from two MWPCs in ^{209}Bi experiment. Comments to this figure are the same as in Fig. 4.

The measured angular distributions for selected fission fragment events were corrected for the efficiency of fission fragment registration. This efficiency was calculated by means of the Monte-Carlo method taking into account following parameters: the electrode wire structure, distances between MWPCs and target, sizes of electrodes and distances between them, sizes of the target and neutron beam, the position (angular) resolution (~ 2 mm).

It should be noted that the measured angular distributions are distorted due to some instrumental systematical effects. Among them are the differential nonlinearity of the delay line chips and the mutual influence (signal crosstalk) of the anodes of two adjacent MWPCs. Thus, additional corrections should be introduced into the measured angular distributions. This correction was obtained by means of additional measurement of $^{252}\text{Cf}(\text{sf})$ placed at the same position as the target of investigated nuclei.

An anisotropy $W(0^\circ)/W(90^\circ)$ of angular distributions of fission fragments in the center-of-mass system were deduced from the corrected $\cos(\theta)$ angular distributions in the laboratory system ($\cos(\theta)$ bins were equal to 0.01) by fitting them in the range $0.24 < \cos(\theta) < 1.0$ by the sum of even Legendre polynomials up to the 4-th order. The fitting range and the order of Legendre polynomials were increased in comparison with our previous work [2], where the range $0.4 < \cos(\theta) < 1.0$ and the 2-nd order polynomials were used. It allowed to make a more accurate description of the fission fragment angular distributions. To account for the linear momentum contribution into the measured angular distribution, the measured anisotropies were averaged over two set-up orientations relative to the beam direction (downstream and upstream).

4. Results

The angular distributions of fission fragments in the centre of mass system for ^{233}U are presented in Fig. 7 for two neutron energy intervals, 1.49 ± 0.16 MeV and 15.7 ± 1.4 MeV in comparison with experimental data of the other authors [6, 9, 10]. The results of the data fitting by the sum of even Legendre polynomials up to the 4-th order are also shown in Fig. 7. It is seen that in these examples our results are in a good agreement with the other data. It is worthwhile to note that experimental techniques used by referred authors differ both in fragment detectors and in neutron sources. It may be treated as a convincing proof of accuracy and reliability of our measurement technique and data handling procedure, at least in the neutron energy range below 20 MeV.

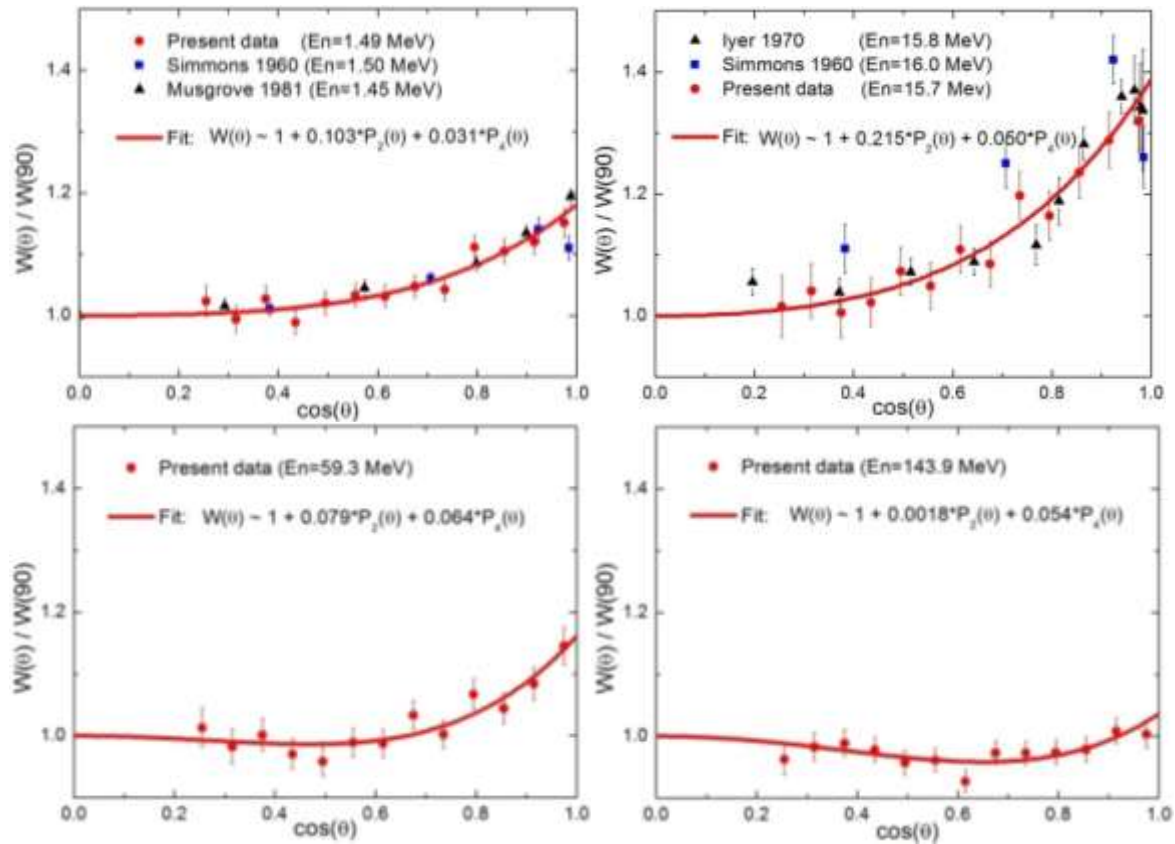


Fig. 7. Example of angular distributions for ^{233}U . The error bars represent statistical uncertainties. Solid line is a result of the fitting by the sum of even Legendre polynomials up to the 4-th order.

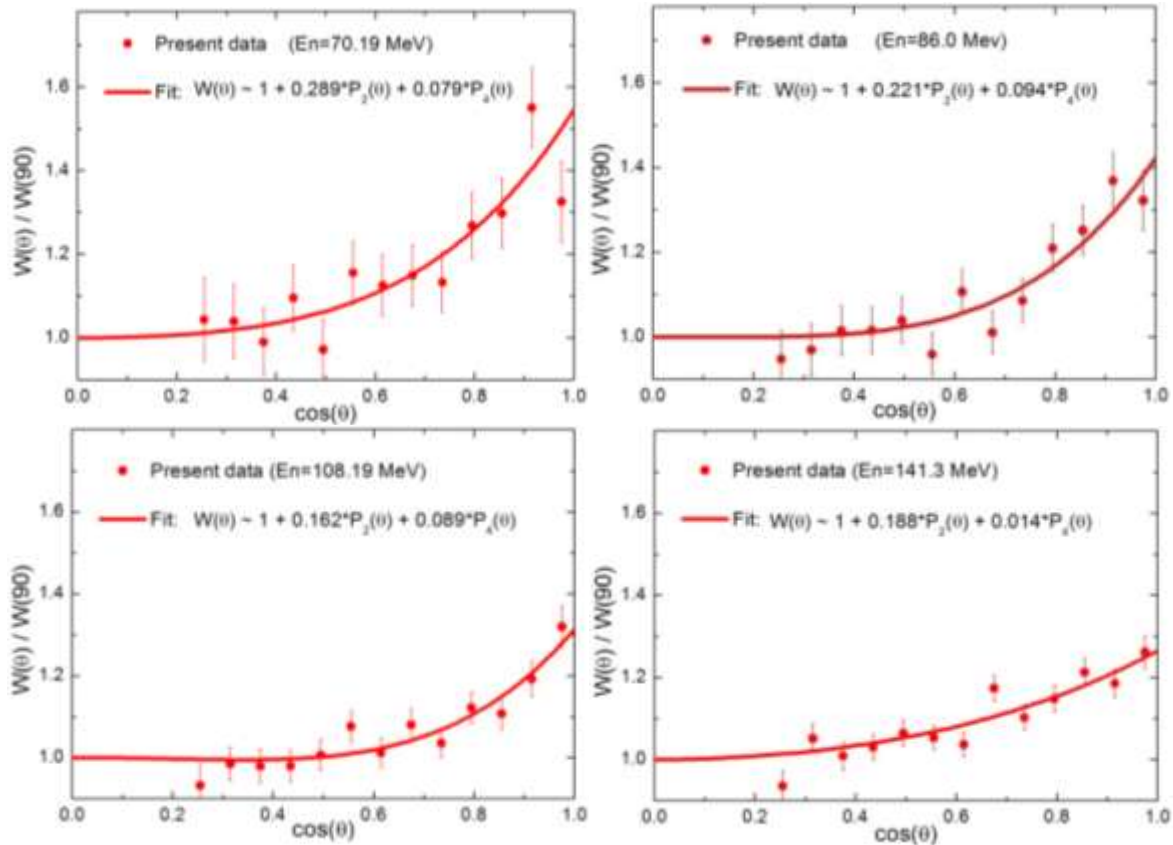


Fig. 8. Example of angular distributions for ^{209}Bi . The error bars represent statistical uncertainties. Solid line is a result of the fitting by the sum of even Legendre polynomials up to the 4-th order.

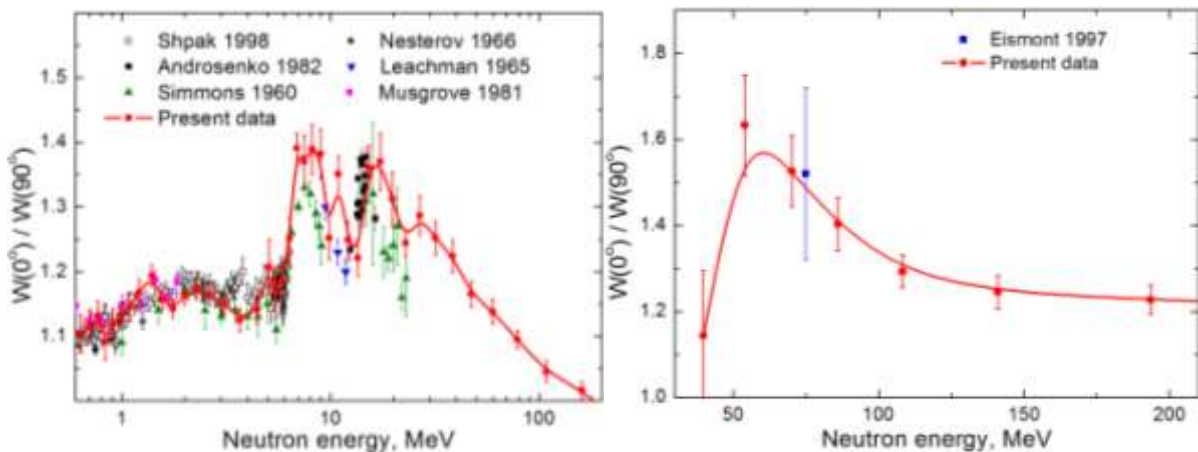


Fig. 9. Anisotropy of fission fragment of ^{233}U (left) and ^{209}Bi (right) compared with the experimental data of other authors ([6, 10–14] for ^{233}U and [7] for ^{209}Bi). The solid curve on each graph is only the eye guide to the experimental data.

As an example of the data obtained for ^{209}Bi , angular distributions of fission fragments in the centre of mass system for some neutron energy intervals are shown in Fig. 8 together with the results of their fit. The anisotropy $W(0^\circ)/W(90^\circ)$ obtained from fitting of the fission fragment distributions measured in present work for ^{233}U and ^{209}Bi in the neutron energy range 1–200 MeV are shown in Fig. 9.

As mentioned above, the results from EXFOR data base [15] on the fission fragment anisotropy for ^{233}U nuclei induced by neutrons with energies exceeding 1 MeV are not numerous. The list of the references contains 9 articles. Apart from our data, the results of 6 former experiments are given on Fig. 8. Three of them deal with the data in the energy range above 10 MeV and only the measurements of Simmons and Henkel [6] cover the range of 1-24 MeV.

In the energy range below 7 MeV, our results agree within experimental uncertainties with the most full data sets by Shpak [14] and Simmons [6] being in fact between them. In the same way, in the energy range 7–24 MeV our data on the average are $4\div 7\%$ above data by Simmons, whereas a discrepancy with the data by Musgrove [10] and Androsenko [13] do not exceeds $\sim 3\%$ and is within experimental uncertainties. Average value of the uncertainties of our data is equal to $2\div 3\%$ in the energy range 20 – 200 MeV.

An experimental data set on the energy dependence of ^{209}Bi anisotropy in the neutron energy range 1–200 MeV has been obtained for the first time. Only one data point measured by Eismont et al [7] is now and this agrees with our data. At the achieved accuracy level, it can be stated that at the energy of $\sim 50\text{--}60$ MeV there is a maximum of the anisotropy equal to 1.6 ± 0.1 followed by a smooth descend with an increase of the neutron energy which resulted in a plateau about 1.2 ± 0.05 of height.

5. Conclusion

To conclude, new experimental data on the angular distributions of fragments from fission of the ^{233}U and ^{209}Bi nuclei by neutrons in the energy range 1–200 MeV are presented. Apart from its significance for applications, these data are of great interest from theoretical point of view. A vastly difference in fission barrier for ^{209}Bi and ^{233}U nuclei could allow to separate the contributions of equilibrium and pre-equilibrium processes to the evolution of nuclear spin alignment during the evaporation cascade. Thus the new directions to study nuclear dynamics at high excitation energies may be open.

Acknowledgments

The authors would like to thank the staff of the Accelerator Department of the PNPI for their permanent friendly assistance and smooth operation of the synchrocyclotron during the experiment.

References

- [1] N.K. Abrosimov, G. Z. Borukhovich, A. B. Laptev, V. V. Marchenkov, G. A. Petrov, O.A. Shcherbakov, Yu.V. Tuboltsev, and V. I. Yurchenko, Nucl. Instrum. Methods Phys. Res. A **242**, 121 (1985).
- [2] A.S. Vorobyev, A.M. Gagarski, O.A. Shcherbakov, L.A. Vaishnena, and A.L. Barabanov, JETP Letters. **102(4)**, 203 (2015).
- [3] L.S. Leong, PhD Thesis, Universite Paris Sud, CERN-Thesis-2013-254.
- [4] E. Leal-Cidoncha, I. Duran, C. Paradela, D. Tarrío, L. S. Leong, L. Tassan-Got, et al., EPJ Web of Conf. **111**, 10002 (2016).
- [5] V. Kleinrath, PhD Thesis, Technischen Universität Wien, 2015.
- [6] J.E. Simmons and R.L. Henkel, Phys. Rev. **120**, 198 (1960).

- [7] V. Eismont, A. Kireev, I. Ryzhov, G. Tutin, K. Elmgren, H. Conde, J. Rahm, J. Blomgren, N. Olsson, E. Ramstrom, in Proceedings of the International Conference on Nuclear Data for Science and Technology, May 19–24, 1997; Trieste, Italy, Conference Proceedings, 59, 658 (1997).
- [8] G.F. Knoll, Radiation Detection and Measurements, NY: J. Wiley, 3rd ed., 2000, p. 190.
- [9] R.H. Iyer, M.L. Sagu, in Proceedings of the Nuclear Physics and Solid State Physics Symposium, December 27–30, 1970; Madurai, India: Nuclear Physics, Vol. 2, p.57 (1970).
- [10] A.R. de L Musgrove, J.W. Boldeman, J.L. Cook, D.W. Lang, E.K. Rose, R.L. Walsh, J. Caruana, and J.N. Mathur, J. Phys. G: Nucl. Phys. **7**, 549 (1981).
- [11] R.B. Leachman and L. Blumberg, Phys. Rev. **137**, B814 (1965).
- [12] V.G. Nesterov, G.N. Smirenkin, and D.L. Shpak, Yadernaya Fizika **4(5)**, 993 (1966).
- [13] Kh.D. Androsenko, G.G. Korolev, and D.L. Shpak, VANT, Ser. Yadernye Konstanty **46(2)**, 9 (1982).
- [14] D.L. Shpak, Physics of Atomic Nuclei, **61(8)**, 1333 (1998).
- [15] N. Otuka, E. Dupont, V. Semkova, B. Pritychenko, A.I. Blokhin, et al., Nuclear Data Sheets, **120**, 272 (2014).